

# An Inverse Free-Electron-Laser Accelerator\*

A.S. Fisher, J.C. Gallardo, A. van Steenberg, S. Ulc, M. Woodle  
National Synchrotron Light Source and Physics Department  
Brookhaven National Laboratory, Upton, NY 11973

J. Sandweiss  
Department of Physics, Yale University, New Haven, CT 06511

Jyan-Min Fang  
Department of Applied Physics, Columbia University, New York, NY 10027

## Abstract

Recent work at BNL on electron acceleration using the Inverse Free-Electron Laser (IFEL) has considered a low-energy, high-gradient, multi-stage linear accelerator. Experiments are planned at BNL's Accelerator Test Facility using its 50-MeV linac and 100-GW CO<sub>2</sub> laser. We have built and tested a fast-excitation wiggler magnet with constant field, tapered period, and overall length of 47 cm. Vanadium-Permendur ferromagnetic laminations are stacked in alternation with copper, eddy-current-induced, field reflectors to achieve a 1.4-T peak field with a 4-mm gap and a typical period of 3 cm. The laser beam will pass through the wiggler in a low-loss, dielectric-coated stainless-steel, rectangular waveguide. The attenuation and transverse mode has been measured in waveguide sections of various lengths, with and without the dielectric. Results of 1-D and 3-D IFEL simulations, including wiggler errors, will be presented for several cases: the initial, single-module experiment with  $\Delta E = 39$  MeV, a four-module design giving  $\Delta E = 100$  MeV in a total length of 2 m, and an eight-module IFEL with  $\Delta E = 210$  MeV.

## I. IFEL ACCELERATOR DESIGNS

An inverse free-electron laser (IFEL) accelerates an electron beam through its interaction with high-power laser radiation and a periodic wiggler field. This concept has been pursued at Brookhaven National Laboratory for several years [1-4], most recently in the form of low-energy ( $\leq 1$  GeV), high-gradient, multistage, linear accelerators [5].

Three sets of IFEL parameters are presented in Table 1. All use constant-field wigglers (described in the following section), assembled in 60-cm-long modules. In an initial demonstration of IFEL acceleration [6], a single-stage IFEL will be tested with the 50-MeV electron beam at Brookhaven's Accelerator Test Facility (ATF), which offers a high-brightness 50-MeV electron beam and a high-power picosecond CO<sub>2</sub> laser. Assuming that a 200-GW peak power in a 6-ps pulse will then be available (20 GW in 30 ps has been demonstrated to date, but shorter pulses with higher powers are under development), an acceleration gradient of 83 MV/m should result. Extending this design to eight modules and higher laser power gives an exit energy of 257 MeV. A third set of parameters [7] responds to the challenge presented at the Port Jefferson Workshop on Advanced Accelerator Concepts (June 1992), for an energy increase of 100 MeV in a total length of 2 m, by using four modules and a relatively modest laser power of 100 GW.

## II. FAST-EXCITATION WIGGLER

To maintain synchronism as an electron accelerates in a laser field with a constant wavelength  $\lambda_l$ , the wiggler must be tapered. The taper can be accomplished while holding

the wiggler parameter  $K_w$ , the period  $\lambda_w$ , or the field  $B_w$  fixed. The choice is restricted by the maximum practical wiggler field and the minimum wiggler period. The maximum rate of acceleration, averaged over the full accelerator length, is obtained for a constant- $B_w$  accelerator [5], and this choice is made for the IFELs in Table 1. Although such a structure could be constructed using permanent magnets, the variable period would be costly and difficult to adjust. Instead, we have developed a fast-excitation electromagnet [8-10] with stackable, geometrically alternating substacks of identical ferromagnetic (Vanadium Permendur, VaP) laminations, assembled in  $(\lambda_w/4)$  thickness substacks separated by nonmagnetic laminations (Fig. 1). Four straight conductive rods, parallel to the axis and interconnected only at the ends of the assembly, constitute the single loop that drives the wiggler. The stacks are easily assembled, are compressed by simple tie rods, and allow any combination of wiggler periods. A dramatic improvement results from using copper for the nonmagnetic laminations, so that the induced fields from the eddy currents uncouple the wiggler's "up" fields from the "down" fields. These "field reflectors" significantly enhance the maximum achievable field on axis.

Both two-dimensional mesh computations (POISSON) and measurements of short wigglers were used to develop the lamination design. Reference [11] presents measurements of a full-length prototype with a tapered period. The wiggler is able to satisfy the requirements of Table 1. Measurements with a constant period of 3.75 cm [12] found an rms field error of under 0.15% and low harmonic content (3% in the 3<sup>rd</sup> harmonic).

## III. CO<sub>2</sub> LASER WAVEGUIDES

Since the wiggler gap is 4 mm, the maximum practical inside diameter for a beam pipe through the wiggler is 3 mm. If a Gaussian laser beam is focused to a 1-mm radius  $\omega_0$  (where the power drops by  $e^{-2}$ ), then the corresponding Rayleigh length  $z_R$  is 30 cm. Waveguiding can occur even in the 47-cm length of the wiggler for the single-stage IFEL, since the free-space beam radius  $\omega(z)$  will exceed the aperture of the waveguide. In a multistage IFEL, waveguiding will be unavoidable—and helpful in confining the beam. Consequently, we are investigating the mode structure and attenuation in CO<sub>2</sub>-laser waveguides.

Our present design uses rectangular stainless-steel guides, with an inside cross section of 2.8 mm  $\times$  2.8 mm. Stainless has good vacuum properties and a conductivity low enough to allow penetration of the pulsed wiggler field. To reduce the expected attenuation, some of the test waveguides were prepared (following Zakowicz [13]) with a 1/4-wavelength dielectric coating (germanium) deposited on two opposite inner walls, in order to reduce surface currents. Subsequently,

\*Work performed under the auspices of the U.S. Department of Energy, under contract DE-AC02-76CH00016.

MASTER

DISTRIBUTION OF THIS DOCUMENT IS UNLIMITED

it was realized that this model strictly applies at lower frequencies, where the metal walls can be treated as nearly perfect conductors. At infrared wavelengths and glancing angles, the metal behaves mostly as a dielectric, and the wall losses are greatly reduced, even without the germanium.

To investigate coupling into the waveguides, transmission loss, and transverse mode structure, eight test guides were built, half with the germanium coating. Six guide sections were 10-inches (254-mm) long; two were 5-inches (127-mm) long. All had precision alignment pins and sockets to permit accurate assembly of lengths of up to 35 inches (889 mm) of either coated or uncoated guide. The beam was focused to a Gaussian waist with an adjustable radius at the entrance to the first guide. The beam profile was measured using a pyroelectric vidicon TV camera and a digital frame grabber.

The coupling tests demonstrated optimum coupling near a waist radius of 1.0 mm. The transmission (including both coupling and attenuation losses) ranged between 80 and 95%, measured with lengths from 10 to 35 in, for entering waists of 1.0 and 1.3 mm, and for both coated and uncoated guides. In all cases, the transmission of the coated guide was  $\approx 2\%$  greater than the uncoated guide. For the longest length tested (35 in), the best result was 88% for the coated guide with a 1-mm entering beam radius.

To measure the transverse beam profile versus distance, the camera was placed within a few millimeters of the exit for guides of various lengths. Fig. 2 shows that when no guide was present, the beam diverged according to  $z_R$ , but within a guide, the beam radius decreased and oscillated about a smaller value, suggesting that some of the energy was in higher-order modes. The beam sizes were not the same for the coated and uncoated guides. Any misalignment of the beam entering the guides or of the junctions between guide sections produced a mode that was not symmetric. The transmission was much less sensitive to alignment.

The laser power must be efficiently coupled into the desired mode. Approximating with an overlap integral, Zakowicz [13] predicted a coupling efficiency of 95% for a beam focused at the guide entrance to a diameter equal to 71% of the guide aperture. To determine the transition region over which the mode becomes established, we performed a series of 2-D ( $xz$ ) scalar diffraction calculations to find the fields propagating from the coupling aperture. The mode pattern transforms from the input Gaussian to a stable field distribution over a distance which is comparable to  $z_R$ . For our waist sizes, after the mode has stabilized (in about 50 cm), the amplitude typically fluctuates by  $\pm 5\%$  and the phase by  $\pm 0.05$  radian, due to a coupling into high-order modes. These calculations suggest a 90% coupling efficiency into the desired mode, but because of the 2-D scalar approximation, the coupling into the real waveguides may not be as pure.

#### IV. IFEL SIMULATIONS

To model the acceleration process in a waveguide IFEL, we have developed a 1-D particle simulation code incorporating self-consistently the longitudinal electron dynamics and the laser field. The code also takes into account the properties of a realistic electron beam, i.e., finite radius, emittance and energy spread. Subsequently, the multiparticle-simulation linac code PARMELA [14] was modified to simulate the full 3-D aspects of the IFEL interaction. The electron beam dynamics include: (a) an arbitrary initial electron distribution in "trace"

Table 1: Simulation parameters for the single-module IFEL experiment, an 8-stage IFEL, and an IFEL with  $\Delta E = 100$  MeV.

	Single	8-Stage	100 MeV	
<b>Electron Beam</b>				
Injection energy	48.9	48.9	49	MeV
Exit energy	88.0	256.9	150	MeV
Mean gradient	33	53	50	MV/m
Charge	1	1	1	nC
Peak current	100	100	100	A
Emittance $\epsilon_n$ ( $\sigma$ )	$7\pi$	$7\pi$	$7\pi$	$\mu\text{m}$
Radius ( $\sigma$ )	0.3	0.3	0.3	mm
<b>Wiggler</b>				
Number of modules	1	8	4	
Module length	60	60	60	cm
Total wiggler length	47	395	200	cm
First period	2.86	2.86	2.86	cm
Last period	4.32	9.08	6.29	cm
Gap	4	4	4	mm
Peak field	1.25	1.25	1.25	T
<b>Laser</b>				
Power	200	620	100	GW
Peak electric field	13.6	24	9.6	GV/m
Wavelength	10.2	10.2	10.2	$\mu\text{m}$
Pulse length	6	6	6	ps

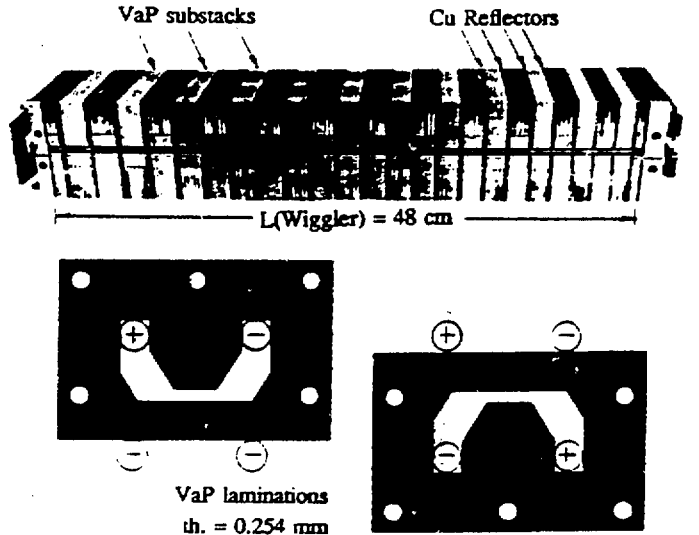


Figure 1: The fast-excitation, variable-period wiggler. The lower portion shows the VaP laminations configured for the two field polarities.

space ( $x, dx/dz, y, dy/dz$ ) determined by the Twiss parameters  $\alpha_x, \beta_x, \alpha_y, \beta_y$  and the transverse emittances  $\epsilon_x$  and  $\epsilon_y$ ; (b) an arbitrary longitudinal initial electron distribution in phase  $\phi$  and energy  $W$ ; (c) a realistic piecewise-constant tapered wiggler, allowing for both horizontal and vertical focusing.

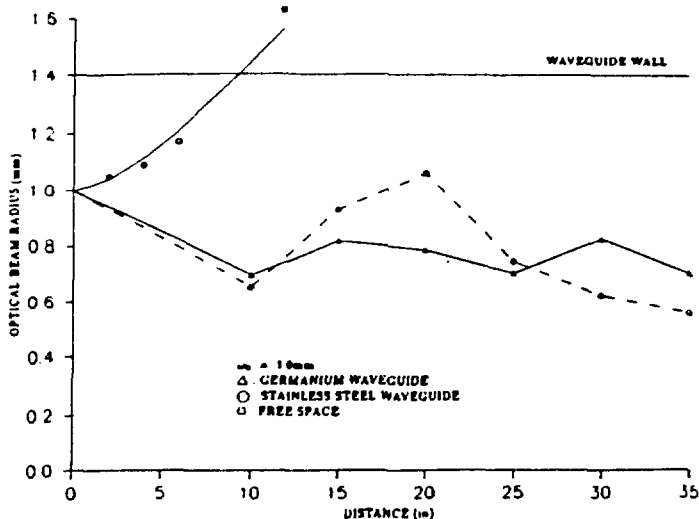


Figure 2: Beam radius  $w$  at the exit of stainless-steel waveguides of various lengths, with and without a germanium coating, for beam waist radius  $w_0$  of 1.0 mm at the guide entrance. The radius without a waveguide is also shown.

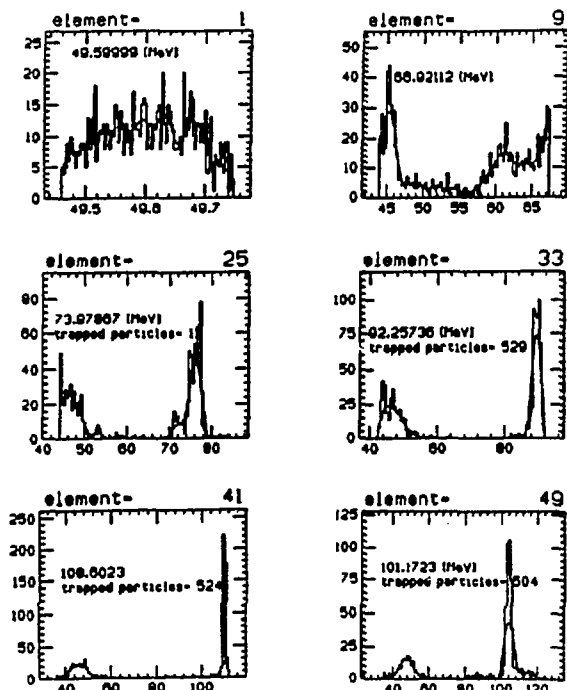


Figure 3: A 3-D simulation of the evolution of the energy spectrum in the early portion of the multistage accelerator.

The results of these calculations are given more fully in Reference [7]. The transverse phase space at the end of the wiggler shows some emittance growth in the horizontal plane and two well defined groups of electrons (accelerated

and non-accelerated) in the vertical plane; the emittances are comparable to the initial value. The evolution of the energy spectrum along the wiggler, in Fig. 3, clearly illustrates the fraction of accelerated electrons ( $\approx 50\%$ ).

For the eight-stage IFEL of Table 1, the 1-D simulation code was used to optimize the sequence of tapered wigglers for a given laser power, resonance phase angle and peak wiggler field. The vertical transverse focusing action of the planar wiggler was taken into account. Instead of shaping the wiggler poles for horizontal focusing, external focusing was added.

## V. CONCLUSION

The study of the IFEL accelerator is continuing with near-term emphasis on low-loss guide development, transverse and longitudinal phase space transport and the further optimization of a multimodule 1-GeV accelerator. For a single demonstration stage, aimed at approximately doubling the beam energy, a  $\text{CO}_2$  laser power of  $10^{11}$  W is satisfactory. A cascaded IFEL accelerating to 1 GeV would require a laser power of  $10^{12}$  W to make the overall device technically competitive.

We wish to acknowledge the assistance of T. Romano and J. Armendaris (wiggler measurements), and of S. Coe and M. Weng (waveguide measurements).

## VI. REFERENCES

\*U.S. Department of Energy contract DE-AC02-76-CH00016.

1. R.B. Palmer, *J. Appl. Phys.* **43**, 3014 (1972).
2. C. Pellegrini, P. Sprangle, W. Zakowics, *Int. Conf. on High-Energy Accelerators* (1983).
3. E.D. Courant, C. Pellegrini, W. Zakowics, *Phys. Rev. A* **32**, 2813 (1985).
4. E. Courant, J. Sandweiss, BNL-38915.
5. A. van Steenbergen, *Experimental Program, ATF*, BNL-41664 (1988); "IFEL Accelerator Demonstration Stage," BNL-43702 (1989).
6. E. Courant et al., "Inverse Free Electron Laser (IFEL) Accelerator Development," *ATF Users Meeting*, Oct. 1991, BNL-47000, CAP 81-ATF-91P, ed. H.G. Kirk, p. 235.
7. A. Fisher, J. Gallardo, J. Sandweiss, A. van Steenbergen, "Inverse Free Electron Laser Accelerator," BNL-47974, to be published in *Third Workshop on Advanced Accelerator Concepts*, Port Jefferson, NY, June 1992.
8. A. van Steenbergen, J. Gallardo, T. Romano, M. Woodle, "Fast Excitation Wiggler Development," *Workshop on Prospects for a 1-Å FEL*, Sag Harbor, NY, April 1990, BNL-52273, ed. J. Gallardo, p. 79.
9. A. van Steenbergen, U.S. Patent Application 368618, June 1989, issued Aug. 1990.
10. A. van Steenbergen, J. Gallardo, T. Romano, M. Woodle, "Fast Excitation Variable Period Wiggler," *1991 IEEE Particle Accelerator Conf.*, San Francisco, CA (IEEE, Piscataway, NJ, 1991), p. 2724.
11. J. Armendaris, J. Gallardo, T. Romano, A. van Steenbergen, "Fast Excitation Wiggler Field Measurement Results," BNL-47928, August 1992.
12. J.C. Gallardo, T. Romano, A. van Steenbergen, "Magnetic Performance of a Fast Excitation Wiggler," BNL-48675, March 1993.
13. W. Zakowics, *J. Appl. Phys.* **55**, 3421 (1984); BNL-34347.
14. L. Young, "PARMELA," 1991 version, private communication.

## **DISCLAIMER**

**This report was prepared as an account of work sponsored by an agency of the United States Government. Neither the United States Government nor any agency thereof, nor any of their employees, makes any warranty, express or implied, or assumes any legal liability or responsibility for the accuracy, completeness, or usefulness of any information, apparatus, product, or process disclosed, or represents that its use would not infringe privately owned rights. Reference herein to any specific commercial product, process, or service by trade name, trademark, manufacturer, or otherwise does not necessarily constitute or imply its endorsement, recommendation, or favoring by the United States Government or any agency thereof. The views and opinions of authors expressed herein do not necessarily state or reflect those of the United States Government or any agency thereof.**